

Metasurface-based Modulation with Enhanced Interference Resilience

Yijia Liu, Nan Qi, Zhibo Pang, *Senior Member, IEEE*, Xinyu Zhang, Qihui Wu, *Senior Member, IEEE*, Shi Jin, *Senior Member, IEEE*, Kai-Kit Wong, *Fellow, IEEE*

Abstract—Reconfigurable Intelligent Surfaces (RISs) have great potential for Internet of Things (IoT) applications due to their cost-effectiveness and energy-efficiency. However, under the application of RIS, current RIS systems cannot actively predict and avoid interference, as evolving interference signals can dynamically change their frequency bands. To address this issue, we develop a learning-based dynamic RIS spectrum access scheme to avoid interference and enhance wireless transmission reliability. An intelligent metasurface-based modulation (MM) is designed for generating and reflecting anti-interference radio-frequency signals. Specifically, a Dyna-Q algorithm is employed at the RIS controller to learn the frequency of interference signals, which is used to determine the frequency of the carrier signals. Experiments are conducted on the proposed RIS demo system to evaluate its anti-interference capability, and the results show that our scheme leads to an increase of at least 50% in the system throughput. These numerical results demonstrate the effectiveness of proposed scheme.

Index Terms—Reconfigurable intelligent surfaces (RIS), metasurface-based modulation (MM), Dyna-Q, dynamic spectrum access.

I. INTRODUCTION

INTERNET of things (IoT) has been a critical paradigm of 5G communication, which is beyond wireless systems, since it provides massive wireless connectivity for a mass of sensor nodes. Despite significant technological advancements, such as the use of ultra-dense networks, multi-input multi-output (MIMO), and mmWave communications, the need for high transmission rates and low energy consumption remains a critical challenge. The concern is that the increased energy consumption and hardware costs associated with these technologies may not be feasible for energy-constrained IoT end users.

Metasurfaces, also called reconfigurable intelligent surfaces (RISs), are considered a green and cost-effective solution to

Yijia Liu, Nan Qi, Qihui Wu, and Xinyu Zhang are in Nanjing University of Aeronautics and Astronautics, Nanjing, China, 210016. Nan Qi is also with National Mobile Communications Research Laboratory, Southeast University, Nanjing 210096, P. R. China (e-mail: nanqi.commun@gmail.com; wuqihui2014@sina.com).

Zhibo Pang is with the Department of Automation Technology, ABB Corporate Research Sweden, 721 78 Vasteras, Sweden, and also with the Department of Intelligent Systems, Royal Institute of Technology (KTH), 114 28 Stockholm, Sweden (e-mail: pang.zhibo@se.abb.com; zhibo@kth.se).

S. Jin is with the National Mobile Communications Research Laboratory, Southeast University, Nanjing 210096, China (e-mail: jinshi@seu.edu.cn).

Kai-Kit Wong is with the Department of Electronic and Electrical Engineering, University College London, London WC1E 7JE, U.K. (e-mail: kai-kit.wong@ucl.ac.uk).

This work was supported in part by the National Key R&D Program of China (No. Grant 2018YFB1800801), Natural Science Foundation of China under Key Project (No. 61931011), the National Natural Science Foundation of China (No. 61827801, 62271253, 61801218, 61901523, 62071223).

the above issue [1]. The features of an RIS can be configured artificially using an external controller, one of the most notable being the realization of intelligent control of the wireless communication environment and breaking the randomness and uncertainty of traditional wireless channels. As such, each reflected signal can be constructively ambient, and the RIS is capable of turning an uncontrollable and unfavorable environment into a controllable and benign entity [2].

Because of its superiority, RIS applications have been widely explored recently, including the Internet of Things and joint sensing [3], large intelligent surface assisted wireless communications [4], and surface-based modulation [5]. The concept of metasurface-based modulation was first introduced in [6], where the authors discussed a practical approach to redesigning conventional network communication paradigms. Afterwards, Miaowen Wen made important contributions to the research by expanding on the concept of metasurface-aided single-RF MIMO and exploring various implementations of spatial modulation. This groundbreaking research highlights the potential of using metasurface-based modulation as a viable alternative to traditional antenna-based modulation. [7]. However, Due to the sharing and open nature of wireless communications, interference has become a critical and major threat in the application of RIS. There are many interference sources with different forms, we focus on frequency-domain anti-interference techniques and can evade interference through frequency hopping [8]. Possible uncontrolled interference sources in these scenarios were likely to seriously damage the communication system performance while escaping from being predicted and avoided in advance. Thus, blindly reflecting both desired and interference signals may lead to a deleterious effect.

To ensure the safety of wireless communication with RISs, we propose an anti-interference scheme in this paper, that is, the metasurface-based modulation (MM) system using dynamic spectrum access. This proposed system can retain the original benefits of MM while improving its ability to avoid interference, ensuring the safety and reliability of wireless communication with RISs. Moreover, an improved Q-learning algorithm is embedded at the receiver side of the RIS system and a reverse acknowledge character (ACK) data link is designed to complete frequency coordination. Note that the proposed algorithm is model-based and works in an online manner [9], i.e., carrier signal frequency decisions can be made through timely interact with the practical environment. We implement our model on a hardware platform and verify the anti-interference performance of the system with experiments.

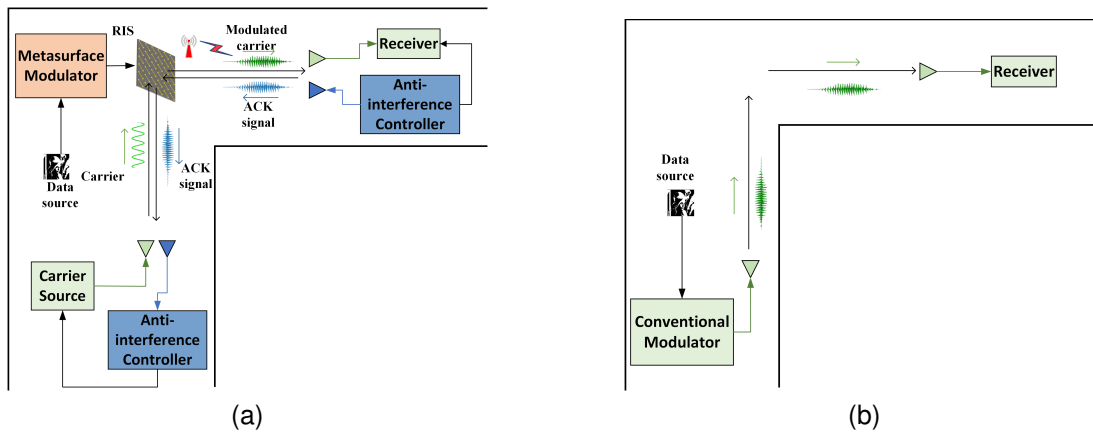


Fig. 1. Metasurface-based modulation system architectures. (a) with RIS, (b) without RIS.

II. SYSTEM MODEL UNDER THE ASSISTANCE OF RIS

Fig. 1 shows a wireless communication system with an RIS being deployed at the corner of an “L”-shaped corridor. Each of the transmitters and receivers is equipped with two horn antennas for full-duplex communication. Modular and carrier in the architecture of MM are separated. We modulate the source information into the RIS in a way of amplitude modulation by controlling the RIS. There are two USRPs at the transmitter side. One of them is used to receive image data and the other is used to send ACK frames that contain the frequency information, which is determined by the algorithm. Note that the ACK frame adopts Gaussian-filtered Minimum Shift Keying (GMSK) modulation. This allows the RIS to assist in the propagation of the ACK signal while performing the function of MM without affecting its demodulation.

A. Architecture of RIS-aided dynamic spectrum access system

The RIS-aided dynamic spectrum access system is placed in an L-shaped corridor to imitate Non-line-of-sight (NLoS) scenario. It can be divided into three parts: the RIS, the carrier source, and the image data receiver. To achieve dynamic spectrum access, two signal links, including the image data transmission link and the ACK signal link, are established with the assistance of the RIS. The details of these three components will be explained in the following sections.

1) *Design of RIS*: The operating frequency band of the RIS is designed in the S-band which is part of the microwave band in the electromagnetic spectrum. Each reflecting element contains a control circuit board for adjusting the reflecting amplitude, triggered by a smart controller such as Field Programmable Gate Array (FPGA). Besides, there is a positive-intrinsic-negative (PIN) diode embedded in each element. By controlling its bias voltage, the PIN can be switched between “On” and “Off” states, making the interface display two different reflecting coefficients accordingly. The RIS designed in this paper operates in the frequency band of 2.12GHz to 2.14GHz. The reflecting coefficient is 0.12 when the PIN diode is on, and 0.98 when off.

2) *Image data transmission link*: The carrier source transmits a sine wave at 2.129GHz by the horn antenna, and then this carrier signal reaches the RIS. Meanwhile, the FPGA

connected with the RIS serves as a control unit and converts the image into the bit stream. It is worth mentioning that we have added a packet head, packet number, and a CRC check code to the data frame to ensure the receiver can successfully recover the image from the bit stream. Then, we use the processed data to control the serial port of the FPGA. The output is 3.3 volts when a “0” bit comes and 0 volts when a “1” bit comes. In this case, the PIN can be switched between the “On” and “Off” states by controlling the bias voltage, causing the coefficient of the RIS to switch accordingly. Thus, the amplitude of the carrier wave can be changed and the 2ASK modulation is realized. At the receiver side, we use a horn antenna to receive signals, and a USRP is utilized for processing. The signal processing blocks provided by GnuRadio are used to complete the demodulation process. The most important component is the M&M (Mueller and Müller) clock recovery block, which is used to perform coherent demodulation. Afterward, the bit stream is sent to the image processing program via a socket that uses the UDP protocol, and the original image is restored.

3) *ACK signal link*: Considering that users need to change frequency to satisfy the dynamic spectrum access, the transmitter and the receiver need a novelty mechanism to coordinate their frequencies. To achieve this, we design an RIS-aided ACK signal link in this paper. Firstly, a USRP is used at the receiver side to perform both the functions of spectrum sensing and ACK signal transmission. Specifically, it continuously obtains spectrum information and transmits it to the computer through an Ethernet cable within a 10MHz frequency band range, with a center frequency of 2.129GHz. Then, the data are processed by the computer and input into the algorithm. The algorithm’s output is the frequency that the system needs to operate on in the next time interval. Since the decision-making module is located on the receiver side, we need to consider how to notify the transmitter of frequency changes. To address this issue, the frequency information is modulated using GMSK and transmitted to the transmitter after being reflected by the RIS. Note that the RIS only changes the signal’s amplitude without affecting the demodulation of the GMSK signal. This means that the forward data transmission and the reverse ACK transmission can be achieved simultaneously



Fig. 2. Setups of the transmitter and the receiver. (a) Transmitter. (b) Receiver.

via RIS. At last, the transmitter demodulates the ACK signal and changes its frequency. A complete dynamic spectrum access process comes to an end. It is worth mentioning that if the ACK signal is jammed, the transmitter can use an LSTM network to predict the current frequency by utilizing the frequency information in the historical ACK signals.

B. Algorithm Design for Dynamic Spectrum Access

In the above NLoS communication scenario, the RIS can ensure the communication quality among users. However, the communication can be significantly affected if there is a malicious interference source in the environment. Assume that the available set of channels to the user is $\{1, 2, \dots, M\}$, and the interference signal source transmits various interference signals in these channels. For instance, the sweeping interference signal source switches channels at regular time intervals to cover all channels. The user's channel selection problem can be modeled as a Markov Decision Process (MDP).

Specifically, $S(f_t(k), f_j(k))$ is used to indicate the finite state space at the k th time interval, where $f_t(k)$ is the channel t selected by the user and $f_j(k)$ is the channel j occupied by the interference signal. Considering that only one channel is used for communication in each time interval, the user can choose a channel from the available channel set $\{1, 2, \dots, M\}$. To solve this MDP problem, the Dyna-Q algorithm, which integrates real and simulated experiences to build a policy, is utilized for decision-making. Both planning and learning are essential in executing the Dyna-Q algorithm. In Reinforcement Learning (RL) terminology, **planning** refers to using simulated experiences generated by a model to discover or enhance an interaction policy in a modeled environment, which is considered model-based. On the other hand, **learning** refers to using actual interactions with the environment to develop a policy, which is considered model-free. In both cases, experience (real or simulated) is used to search for the optimal policy in the state space based on the updates of the value function. The reward function in the Dyna-Q algorithm is set as follows,

$$Q(s, a) = Q(s, a) + \alpha[r + \gamma \max_a Q(s', a) - Q(s, a)], \quad (1)$$

where α is the learning rate, γ is the discount rate, and r is the reward of action a taken by the user in state s . Here we

define a as the action that the user changes its frequency. The Reward r is calculated as follows,

$$r_k = \begin{cases} 0, & a_k = f_j(k+1) \\ 1, & a_k \neq f_j(k+1) \end{cases} \quad (2)$$

where $f_j(k+1)$ is the channel being interfered at the $(k+1)$ th interval. The process of the user avoiding interference is shown in **Algorithm 1**.

Algorithm 1 Dyna-Q algorithm for anti-interference and carrier frequency selection

- Initialize $Q(s, a)$ and $Model(s, a)$
 Loop forever:
 (a) $s \leftarrow$ current state
 (b) $a \leftarrow \epsilon - greedy(s, Q)$
 (c) Take action a , observe resultant reward r and state s'
 (d) $Q(s, a) = Q(s, a) + \alpha[r + \gamma \max_a Q(s', a) - Q(s, a)]$
 (e) $Model(s, a) \leftarrow r, s'$
 (f) Loop repeat n times:
 $s \leftarrow$ previous observed state selected by random
 $a \leftarrow$ random action previously taken in s
 $r, s' \leftarrow Model(s, a)$
 $Q(s, a) = Q(s, a) + \alpha[r + \gamma \max_a Q(s', a) - Q(s, a)]$
-

III. PLATFORM DEMONSTRATION AND RESULT ANALYSIS

A. Platform demonstration

To evaluate the performance of the proposed Reflecting Intelligent Surface (RIS)-assisted dynamic spectrum access system, a series of field experiments have been conducted. The anti-interference gain and the performance improvement brought by the RIS are preliminarily verified.

We selected the L-shaped corridor to establish the NLoS scenario. Fig. 2a shows the position-fixed transmitter side, which consists of two horn antennas, a USRP, and a carrier source. The RIS is located at the corner of the corridor, and the angle between the antenna direction and the normal line of the RIS is 45° . To control the reflection coefficient of the RIS, we first transform the picture into a bit stream and feed it

TABLE I
PARAMETER SETTINGS

Parameter	value
User's available frequency (GHz)	2.124~2.134
User's signal bandwidth (kHz)	400
Transmitter distance (m)	10
Receiver distance (m)	5~10
Antenna gain (dBi)	30
Interference signal power (dBm)	0~15
Interference signal bandwidth (MHz)	2
Center frequency of interference signal (GHz)	2.125, 2.127, 2.129, 2.131, 2.133
Frame name	Number of bits
Packet head	8
Packet sequence number	8
Image data	96
CRC code	32

to the serial port of FPGA. Then, the reflection coefficient of RIS will change depending on the output voltage of the serial port. As a result, when the carrier is reflected by the RIS, the image data will be modulated into the carrier in the 2ASK mode. Fig. 2b shows the receiver side. The initial distance between the receiver and the RIS is 5m, which can be varied in the range of 5 ~ 10m. There are two USRPs at the receiver side, one of which is to sense the spectrum, and the other is connected with two horn antennas to simultaneously receive image data and transmit the ACK signal. Note that there is an interference signal source that can release a sweep signal between the receiver and the RIS. The experimental parameters and the image data packet format are shown in Table I.

B. Result Analysis

The system performance in this NLoS scenario is tested with and without the RIS, respectively. Fig. 3 presents the throughput and packet error rate of the system. It can be seen that without the assistance of the RIS, the packet error rate of the system can reach 80% and the user cannot communicate normally. Instead, the packet error rate drops to 15%, and the throughput is significantly improved with RIS assistance.

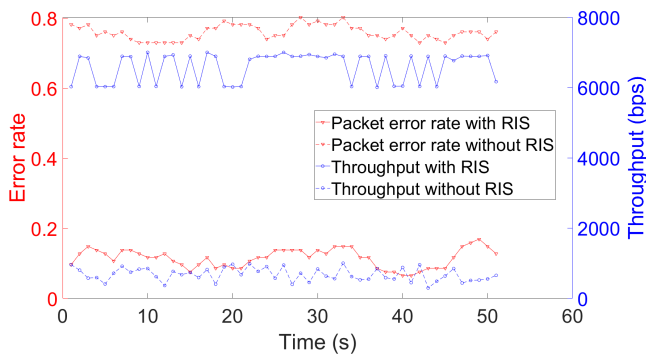


Fig. 3. Performance comparison (with RIS and without RIS)

Fig. 4 displays the system performance after changing the distance between the receiver and the RIS. It can be seen that the packet error and the throughput change gently with different distances and are both maintained at an acceptable level.

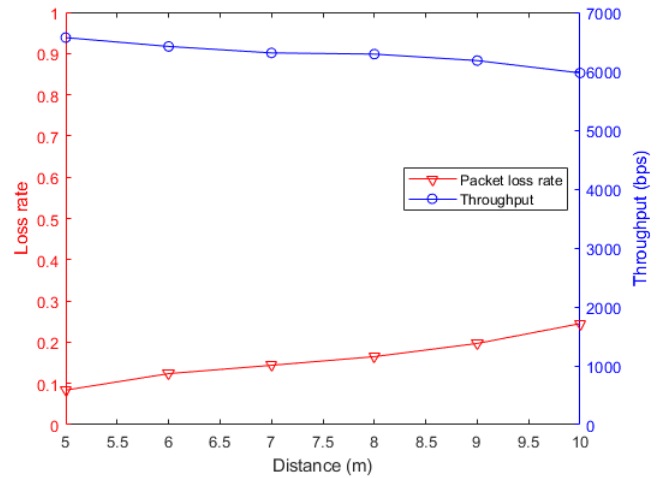


Fig. 4. System performance with different transmitter-receiver distances

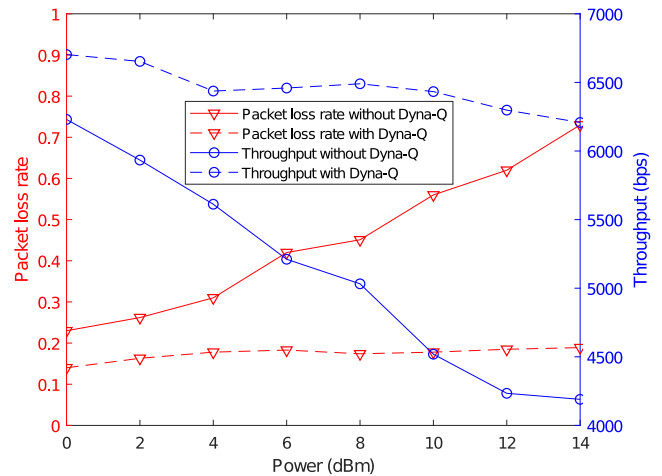


Fig. 5. System performance with/without Dyna-Q under different interference signal powers

To test the impact of interference on the dynamic spectrum access mechanism, we design an interference signal source that can release signals with different powers. The system performance with the interference signal source is shown in Fig. 5. It can be observed that when the dynamic spectrum access mechanism is non-interventional, the packet error rate increases while the throughput decreases.

To counter the effect of the interference signal, the dynamic spectrum access mechanism based on Dyna-Q is designed. As shown in Fig. 5, when the Dyna-Q algorithm gets involved, the packet error rate and the throughput have resumed to a normal level. Fig. 6 provides a more intuitive comparison of image transmission quality with and without dynamic spectrum access. Furthermore, to verify the performance of the Dyna-Q algorithm, we formulate three dynamic spectrum access strategies, which are random frequency selection, Q-Learning, and Dyan-Q, respectively. Fig. 7 shows the convergence performance and speed. Simulation results verify that the Dyna-Q algorithm performs best under the sweep signal.

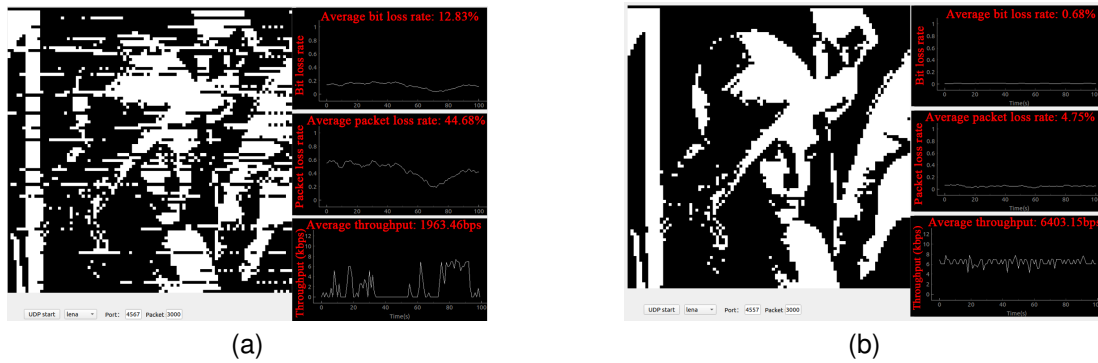


Fig. 6. Quality of image transmission. (a) without dynamic spectrum access, (b) with dynamic spectrum access.

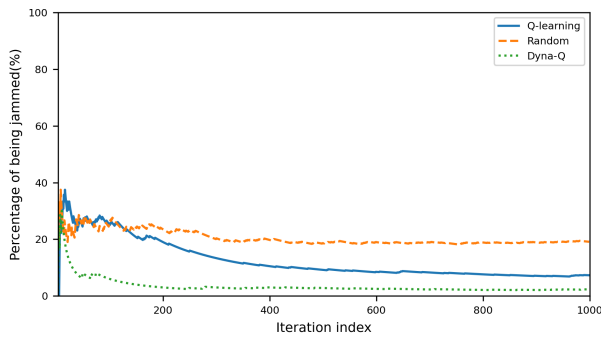


Fig. 7. Convergence performance of three algorithms

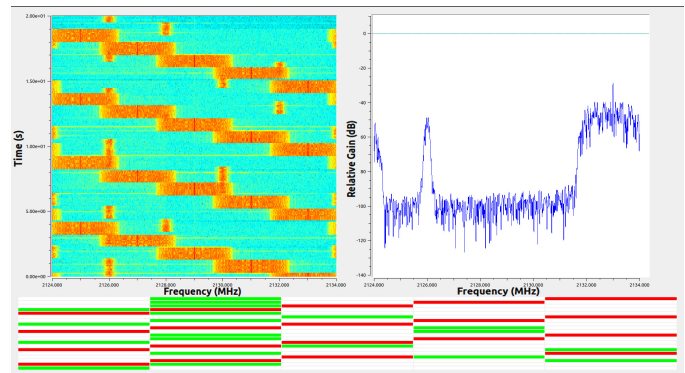


Fig. 8. Graphical user interface

The percentage of being jammed can be reduced to less than 5% compared to random frequency selection, with a faster convergence rate than Q-learning.

To show the impact of the algorithm on system performance more clearly, we design a graphical user interface of spectrum map, as shown in Fig. 8. The interface can be divided into three parts: the spectrum waterfall chart on the upper left, the spectrum chart on the upper right, and the spectrum semantics map at the bottom. All five frequency bands are used, as can be seen in the semantics map. The red rectangle represents the frequency that is being interfered with at the current time slot, while the green rectangle represents the frequency selected by the algorithm. This graph allows us to see that the interference signal and user signal occupy different frequencies at all times, ensuring that the user will not experience any interference.

IV. CONCLUSION

In this paper, a learning-based RIS framework was proposed, where intelligent metasurface modulation for boosting anti-interference signal transmission was designed. An improved online Q-learning algorithm and a reverse ACK data link were introduced to realize frequency coordination. An anti-interference RIS demo platform has been built, on which a series of field experiments have been executed to verify the anti-interference capability. Numerical results demonstrated that under the sweep interference signal, our scheme could improve the user's throughput by at least 50% and reduce the percentage of being jammed to less than 5%.

REFERENCES

- [1] C. Huang, A. Zappone, G. C. Alexandropoulos, M. Debbah, and C. Yuen, "Reconfigurable intelligent surfaces for energy efficiency in wireless communication," *IEEE Transactions on Wireless Communications*, vol. 18, no. 8, pp. 4157–4170, 2019.
- [2] R. M. Di, D. Merouane, P. H. Dinh-Thuy, Z. Alessio, A. Mohamed-Slim, Y. Chau, S. Vincenzo, G. C. Alexandropoulos, H. Jakob, and G. Haris, "Smart radio environments empowered by reconfigurable AI meta-surfaces: an idea whose time has come."
- [3] M. Di Renzo, A. Zappone, M. Debbah, M.-S. Alouini, C. Yuen, J. De Rosny, and S. Tretyakov, "Smart radio environments empowered by reconfigurable intelligent surfaces: How it works, state of research, and the road ahead," *IEEE journal on selected areas in communications*, vol. 38, no. 11, pp. 2450–2525, 2020.
- [4] Y. Han, W. Tang, S. Jin, C.-K. Wen, and X. Ma, "Large intelligent surface-assisted wireless communication exploiting statistical CSI," *IEEE Transactions on Vehicular Technology*, vol. 68, no. 8, pp. 8238–8242, 2019.
- [5] A. E. Canbilen, E. Basar, and S. S. Ikki, "Reconfigurable intelligent surface-assisted space shift keying," *IEEE wireless communications letters*, vol. 9, no. 9, pp. 1495–1499, 2020.
- [6] M. D. Renzo, M. Debbah, D.-T. Phan-Huy, A. Zappone, M.-S. Alouini, C. Yuen, V. Sciancalepore, G. C. Alexandropoulos, J. Hoydis, H. Gacanin *et al.*, "Smart radio environments empowered by reconfigurable AI meta-surfaces: An idea whose time has come," *EURASIP Journal on Wireless Communications and Networking*, vol. 2019, no. 1, pp. 1–20, 2019.
- [7] Q. Li, M. Wen, and M. Di Renzo, "Single-RF MIMO: From spatial modulation to metasurface-based modulation," *IEEE Wireless Communications*, vol. 28, no. 4, pp. 88–95, 2021.
- [8] L. Jia, N. Qi, F. Chu, S. Fang, X. Wang, S. Ma, and S. Feng, "Game-theoretic learning anti-jamming approaches in wireless networks," *IEEE Communications Magazine*, vol. 60, no. 5, pp. 60–66, 2022.
- [9] B. Peng, X. Li, J. Gao, J. Liu, K.-F. Wong, and S.-Y. Su, "Deep dyna-q: Integrating planning for task-completion dialogue policy learning," *arXiv preprint arXiv:1801.06176*, 2018.